Revista Brasileira de Farmacognosia 26 (2016) 352–362

Brazilian Journal of Pharmacognosy
REVISTA BRASILEIRA DE FARMACOGNOSIA
www.elsevier.com/locate/bjp

Original Article

In vivo diabetic wound healing effect and HPLC–DAD–ESI–MS/MS profiling of the methanol extracts of eight *Aloe* species

Abeer M. El Sayed[a], Shahira M. Ezzat[a,*], Moataz M. El Naggar[b], Seham S. El Hawary[a]

[a] *Pharmacognosy Department, Faculty of Pharmacy, Cairo University, Cairo, Egypt*
[b] *Department of Pharmacognosy, Faculty of Pharmacy, Damanhour University, Damanhour City, Egypt*

ARTICLE INFO

Article history:
Received 12 October 2015
Accepted 12 January 2016
Available online 31 March 2016

Keywords:
Aloe
HPLC–DAD–MS/MS
Chemotaxonomic
Anti-inflammatory
Wound healing

ABSTRACT

Genus *Aloe*, Xanthorrhoeaceae, is well distributed all over Egypt, and many species have been used as medicinal plants; mainly reported to prevent cardiovascular diseases, cancer and diabetes. This study attempts to analyze the secondary metabolites in the methanol extract of the leaves of eight *Aloe* species; *A. vera* (L.) Burm. f., *A. arborescens* Mill., *A. eru* A. Berger, *A. grandidentata* Salm-Dyck, *A. perfoliata* L., *A. brevifolia* Mill., *A. saponaria* Haw. and *A. ferox* Mill. growing in Egypt. For this aim HPLC–DAD–MS/MS in negative ion mode was used. Although belonging to the same genus, the composition of each species presented different particularities. Seventy one compounds were identified in the investigated *Aloe* species, of which *cis-p*-coumaric acid derivaties, 3,4-*O*-(*E*) caffeoylferuloylquinic acid and caffeoyl quinic acid hexoside were the most common phenolic acids identified. Aloeresin E and isoaloeresin D, 2′-*O*-feruloylaloesin were the common anthraquinones identified. Lucenin II, vicenin II, and orientin were the common identified flavonoids in the investigated *Aloe* species. 6′-Malonylnataloin, aloe-emodin-8-*O*-glucoside, flavone-6,8-di-*C*-glucosides could be considered as chemotaxonomic markers for the investigated *Aloe* species. The eight *Aloe* species had significant anti-inflammatory activity, in addition to the significant acceleration of diabetic wound healing in rats following topical application of the methanol extracts of their leaves. This is the first simultaneous characterization and qualitative determination of multiple phenolic compounds in *Aloe* species from locally grown cultivars in Egypt using HPLC–DAD–MS/MS, which can be applied to standardize the quality of different *Aloe* species and the future design of nutraceuticals and cosmetic preparations.

Introduction

The genus *Aloe* L. (family Xanthorrhoeaceae, subfamily Asphodeloideae) is an old world genus which comprises more than 400 species, which has centers of diversity in southern and east Africa and Madagascar (Newton, 2004). *Aloe* is used as a traditional medicine for treatment of different diseases, as ingredients of food products and cosmetics (Eshun and He, 2004). Phenolic compounds including chromones, anthraquinones, and pyrones constitute the major secondary metabolites of *Aloe* (Conner et al., 1990; Okamura et al., 1998; Durì et al., 2004). Most of these compounds have been reported to possess several biological activities such as antitumor, antidiabetic and antityrosinase, in addition to the antiulcer activity (Imanishi et al., 1981; Yagi et al., 1987; Beppu et al., 1993; Teradaira et al., 1993). Some components isolated from *Aloe* species were reported to possess anti-inflammatory effect for example; an effective anti-inflammatory cinnamoyl-*C*-glucosyl-chromone has been isolated from *Aloe barbadensis* (Hutter et al., 1996). Moreover, the wound-healing properties of *A. barbadensis* was also reported (Davis et al., 1989).

The phytochemical constituents and bioactivity of *Aloe* spp. have attracted research interest since the trade in 'drug aloes', prepared from the leaf exudate, expanded rapidly in the nineteenth century (Yeats, 1870). Today, the principal sources of these natural products are wild populations of *Aloe ferox* in South Africa, and *Aloe scabrifolia*, *Aloe secundiflora* and *Aloe turkanensis* in east Africa (Oldfield, 2004). Moreover, *Aloe vera*, the source of the leaf parenchyma known as 'aloe gel', is widely cultivated.

Aloe leaves in addition of being of pharmacological importance, their chemistry have systematic significance, particularly at the infrageneric rank. Secondary metabolites profile was used in the evaluation of infrageneric groups such as series *Longistylae*, section *Pachydendron*, section *Anguialoe* and series *Purpurascentes* Salm-Dyck (Van Heerden et al., 1996; Reynolds, 1997; Viljoen and Van Wyk, 2001). Phytochemical data may offer a tool to study the complexity of maculate species, which comprise about 40 species

* Corresponding author.
E-mail: shahira.ezzat@pharma.cu.edu.org (S.M. Ezzat).

http://dx.doi.org/10.1016/j.bjp.2016.01.009

so-named because of their conspicuous leaf markings. Although it is widely regarded as a well-supported group, infrageneric boundaries and species delimitation in the maculate complex are problematic (Grace et al., 2008).

For this purpose we have started a detailed screening of eight *Aloe* species; *A. vera* (L.) Burm. f., *A. arborescens* Mill., *A. eru* A. Berger, *A. grandidentata* Salm-Dyck, *A. perfoliata* L., *A. brevifolia* Mill., *A. saponaria* Haw. and *A. ferox* Mill growing in Egypt; using HPLC coupled to electrospray ionization mass spectrometry (ESI-MS) [HPLC–DAD–ESI–MS/MS] with the aim of identifying unique constituents which may be used as markers with possible chemotaxonomic significance. In addition, to evaluate the diabetic wound healing and anti-inflammatory effects of the eight *Aloe* species in rats using the diabetic wound model and carrageenan-induced paw edema tests.

Experimental

Plant material

The leaves of the eight *Aloe* species, *A. vera* (L.) Burm. f., *A. arborescens* Mill., *A. eru* A. Berger, *A. grandidentata* Salm-Dyck, *A. perfoliata* L., *A. brevifolia* Mill., *A. saponaria* Haw. and *A. ferox* Mill. were collected in April 2014 from El-Orman Garden, Giza, Egypt. The plants were authenticated by Dr. Reem Samir Hamdy, Lecturer of Plant Taxonomy, Botany Department, Faculty of Science, Cairo University, Giza, Egypt. Voucher samples no. 2014422 of the plants were deposited at the Museum of the Pharmacognosy Department, Faculty of Pharmacy, Cairo University.

Extraction

The fresh leaves of the eight *Aloe* species (500 g each) were cut into pieces and extracted with methanol using cold method of extraction (percolation) (4× 2 l) till exhaustion. The methanol extract in each case was filtered, distilled and evaporated under reduced pressure to give 12.65, 12.44, 5.21, 20.02, 6.97, 6.94, 3.86 and 3.96 g of *A. vera*, *A. arborescens*, *A. eru*, *A. grandidentata*, *A. perfoliata*, *A. brevifolia*, *A. saponaria* and *A. ferox*, respectively.

Qualitative determination of the phenolic contents of *Aloe* leaves using HPLC–DAD–ESI-MS/MS

Sample preparation

Aloe extracts were separately dissolved in HPLC grade methanol in a concentration of 10 mg/ml then filtrated through a syringe-filter-membrane. Aliquots of 5 μl were injected into the LC–DAD/MS Dionex Ultimate 3000 HPLC (Germany), used for performing the analyses.

HPLC conditions

The method of El Maggar (2012) was employed. HPLC apparatus (Hewlett-Packard 1100, Waldbronn, Germany) with a quaternary pump and on line degasser was employed for analysis. A thermostatted column compartment with an auto sampler, a photodiode array detector (DAD). The separation was performed on Eclipse XDB C18 column (50 mm × 2.1 mm, 1.8 μm, Agilent Company, USA). 1100 ChemStation software was used. The mobile phase was composed of two solvents, A: methanol and B: 0.2% formic acid in water. Gradient elution profile was performed: 0 min, A:B 10:90; 36 min, A:B 100:0; 40 min, A:B 100:0. Chromatography was performed at 30 °C with a flow-rate of 0.2 ml/min. UV traces were measured at 290, 254 and 350 nm and UV spectra (DAD) were recorded between 190 and 900 nm.

Mass spectrometric conditions

Electrospray ionization (ESI) interfaced Bruker Daltonik Esquire-LC ion trap mass spectrometer (Bremen, Germany) and an Agilent HP1100 HPLC system were used for HPLC–MS analysis. An autosampler and a UV–vis absorbance detector were used. The ionization parameters were as follows: capillary voltage 4000 V, end plate voltage −500 V; nebulizing gas of nitrogen at 35.0 p.s.i.; drying gas of 10 l/min nitrogen at 350 °C. Mass analyzer scanned from 15 to 1000 u. The MS–MS spectra were recorded in auto-MS–MS mode. The fragmentation amplitude was set to 1.0 V. MS2 data. Mass spectra were simultaneously acquired using electrospray ionization in the negative ionization mode.

Chemicals

Dermazine® cream (silver sulfadiazine) was used as a standard wound healing drug. Indomethacin (Indomethacin)®, Eipico, Egyptian Int. Pharmaceutical Industries Co. was used as a standard anti-inflammatory drug; Carrageenan and Alloxan (Sigma Co., USA).

Evaluation of the biological activity

Animals

Adult male rats of Sprague-Dawley strain (130–150 g) were obtained from the laboratory animal facility of the National Research Center, Dokki, Giza. Animals were housed in steel cages under standard conditions and fed with standard pellets and water *ad libitum*. All experimental procedures were conducted in accordance with internationally accepted principles for laboratory animal use and care, and were approved by the Ethics Committee (No. 9-031) in accordance with recommendations for the proper care and use of laboratory animals (NIH Publication No. 80-23; revised 1978).

Evaluation of anti-inflammatory activity

The method of Winter et al. (1962) was adopted, where ten groups of rats (each of six) were used, eight groups served as the test groups, each of them was administered a single oral dose of each of the methanol extract of the eight tested species (A_1–A_8) in a dose of 250 mg/kg body weight. The dose of the extracts was determined as 250 mg/kg on the basis of a preliminary short-term pilot study with a range of variable doses. The other two groups, one of them received 1 ml saline and served as a negative control group and the other received Indomethacin, 20 mg/kg body weight as a reference drug. Drugs were orally administered 1 h prior to carrageenan injection. Edema was induced in the rat right hind paw by subcutaneous injection of 0.1 ml of 1% carrageenan suspension in saline. Thickness of the right hind paw (mm) was measured immediately before and 1, 2, 3 and 4 h post carrageenan injection with a micrometer caliber. The results are considered significant when they are different from zero time at $p < 0.05$.

In vivo *diabetic wound healing study*

A previously established chemically induced type II diabetic foot ulcer animal model was employed in this study (Lau et al., 2008). For those diabetic rats (plasma glucose levels ≥250 mg/dl, samples collected from tail veins), sixty rats were divided into ten groups, a standardized wound area (2 mm × 5 mm skin in full thickness removed) was induced on the dorsal surface of the right hind foot of rats under anaesthetization with phenobarbitone. Eight groups were treated topically with each of the methanol extract of each of the eight tested species by topical application on the wounded area. The other two groups act as a negative (untreated group) and a positive control group (treated with Dermazine® cream). The treatment

in each group was started at the day of the operation and continued till the 10th day. The wounds were covered with appropriate dressings, which were changed regularly. On changing the dressings, wounds were inspected, measured and photographed. The wound areas were measured while animals were under anesthesia on 2nd, 6th and 10th day after surgery. The progressive changes in wound area were measured by a plantimeter, wound contraction were expressed as percentage reduction of original wound size [wound area at day 0 – wound area at day *n*/wound area at day 0] × 100.

Statistical analysis

The statistical comparison of difference between the control group and the treated groups was carried out using two-way ANOVA followed by Duncan's multiple range test.

Results and discussion

The classes of compounds were recognizable from their characteristic UV spectra, which were identified based on the HPLC–DAD–ESI–MS/MS data and subsequent confirmation by comparison with literature data. The chromatographic and spectroscopic data summarized in Table 1 and Fig. 1.

Chromatographic peaks annotation

Phenolic acids

Hydroxycinnamic acids such as esters of quinic acid were detected as about 10 compounds in *A. eru*, *A. grandidentata*, *A. brevifolia*, *A. saponaria* and *A. ferox* extracts condensed either with caffeic, ferulic or coumaric acids. The detected mass $[M-H]^-$ at *m*/*z* 651, 515, 408, 353, 601, 620, 529, 516, 613 and 483 of the peaks, 1 (Rt 118.2 s), 2 (Rt 248 s), 8 (Rt 716 s), 10 (Rt 728 s), 11 (Rt 796 s), 16 (Rt 875.2 s), 17 (Rt 888 s), 23 (Rt 942.1 s), 31 (Rt 976 s), and 38 (Rt 1025), respectively. Those peaks showed the characteristic base peak of quinic acid, ferulic acid, coumaric acid and caffeic acid at *m*/*z* 191,193,163 and 179, respectively.

Regarding dicaffeoylquinic acids, peak 2 (Rt 248 s) showed *m*/*z* at 515 $[M-H]^-$, this was identified as 3,4-di-*O*-(*E*)-caffeoylquinic acid (**1**). Peak 17 (Rt 888 s) was identified as 3-*O*-(*E*)-caffeoyl-4-*O*-feruloylquinic acid (**2**), it showed $[M-H]^-$ at *m*/*z* 529 ($C_{26}H_{26}O_{12}$) in the negative ionization mode. This parent ion was fragmented in product ions at *m*/*z* 367 base peak, produced by the loss of a caffeoyl unit, and *m*/*z* 353, produced by the loss of a feruloyl unit. Caffeoylferuloylquinic acid was detected in *A. arborescens*, *A. eru*, *A. grandidentata* and *A. perfoliata* only. Peak 30 (Rt 970.2 s) showed $[M-H]^-$ at *m*/*z* at 499 in the negative ionization mode. Peak 30 showed daughter ions at *m*/*z* 353, *m*/*z* 191 (base peak), *m*/*z* 179 and *m*/*z* 163. This compound was identified as **3**-*O*-(*E*)-caffeoyl-5-*O*-*p*-coumaroylquinic acid (**3**) (Gouveia and Castilho, 2011), this compound was only detected in *A. vera*, *A. arborescens* and *A. perfoliata*.

Peak 23 (Rt 942.1 s) was identified as caffeoylquinic hexoside (Gobbo-Neto and Lopes, 2008) and peak 16 (Rt 875.2 s) was likely identified as *trans p*-coumaric derivative.

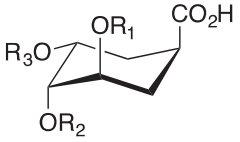

1 R_1=R_2= *E*-caffeic acid; R_3=H
2 R_1= *E*-caffeic acid; R_2=ferulic acid; R_3=H
3 R_1= *E*-caffeic acid; R_2= H; R_3=*p*-coumaric acid

Polyketides

Mass spectrum of peak 3 (Rt 599 s) showed $[M-H]^-$ at *m*/*z* 393 which showed a daughter ion at *m*/*z* 247 due to the loss of 90 amu as a result of a cross-ring cleavage in the hexosidic part involved in the formation of the ion at 247. This fragmentation was previously reported for deprotonated and protonated flavonoid *C*-glycosides. Common ions were also noted at *m*/*z* 41 and 59 and a neutral loss of 120 amu was observed. This compound was identified as aloesin (**4**, aloeresin B), which was detected in *A. grandidentata* and *A. perfoliata*. This compound was previously reported in leaves of *A. castanea* (Van Heerden et al., 2000). Aloesin A and B are *Aloe* resin with no purgative action. Aloesin B is a chromone-*C*-glucoside, where aloesin A is a *p*-coumaric acid ester of aloesin B.

The negative mode ESI-MS spectrum of peak 13 (Rt 841.9 s) showed a strong $[M-H]^-$ parent ion at *m*/*z* 595 corresponding to the caffeoyl ester of 5-hydroxyaloin A. Fragment ions at *m*/*z* 433 and 271 were observed in MS^2 consistent with the loss of caffeoyl and caffeoyl plus carbohydrate moieties from the parent molecules, respectively. A further fragment ion with *m*/*z* 314 corresponds to the loss of ester group together with a four carbon fragment of the carbohydrate moiety. Caffeoyl ester of 5-hydroxyaloin A was noted in *A. vera*, *A. arborescens* and *A. grandidentata*.

Aloeresin C (**5**) was detected as peak 19 (Rt 915.8 s) showing $[M-H]^-$ at *m*/*z* 702, 541 (703-$C_6H_{10}O_5$), corresponding to aloeresin A (**6**), *m*/*z* 394 equivalent to aloesin and *m*/*z* 232 corresponding to aloesone. Aloeresin C represent the first example of *C*,*O*-diglucoside of 5-alkylchromoneaglycone detected only in *A. vera*, *A. arborescens*, *A. perfoliata*, and *A. brevifolia*.

Mass spectra of peak 29 (Rt 962.6 s) showed $[M-H]^-$ at *m*/*z* 409.1 was identified as aloenin (**7**, 4-methoxy-6-(2-*β*-D-glucopyranosyloxy-4-hydroxy-6-methylphenyl)-2-pyrone). This compound was detected only in *A. eru*. Aloenin B (**8**, peak 58, Rt 1290 s), is a bitter glucoside previously isolated from *Aloe* leaves and found to exhibit an inhibitory action on gastric juice secretion of rats (Hirata and Suga, 1978). This compound was detected in *A. vera*, *A. arborescens*, *A. eru* and *A. grandidentata*.

The negative mode ESI-MS spectrum of peak 33 (Rt 998 s) showed a strong $[M-H]^-$ parent ion at *m*/*z* 433. MS^2 of the compound yielded a daughter ion at *m*/*z* 271 resulted from the loss of a sugar moiety ($C_6H_{11}O_5$) from the parent molecules. A moderately abundant ion at *m*/*z* 313 probably results from the loss of a ($C_4H_8O_4$) fragment from the $[M-H]^-$ parent ion. Compound 33 was identified as 5-hydroxyaloin A (**9**) (Holzapfel et al., 1997) and this was only detected in *A. grandidentata* and *A. perfoliata*.

Peak 34 (Rt 1011.9 s) showed $[M-H]^-$ at *m*/*z* 505 was identified as 6′-malonylnataloin (**10**, nataloin), compound considered of great importance in systematic discrimination of different *Aloe* species. 6-Malonylnataloin is a putative marker for African taxa in the maculate species complex, although it was not detected in *Aloe maculata* [*A. saponaria*]; commonly known as the Soap *Aloe* or Zebra *Aloe*; which is a Southern African species of *Aloe*. On the contrary, nataloin has been observed in non-maculate species as diverse in form and infrageneric position as *A. vera*, *A. arborescens*, *A. eru*, *A. grandidentata*, *A. brevifolia* and *A. ferox*; those are related east African species and nataloin may therefore, serve as a phytochemical marker for them (Wabuyele, 2006). Comparative data indicated that the anthrone *C*-glycoside, 6-malonylnataloin (7-hydroxychrysaloin 6-*O*-malonate) is typical of maculate species in East Africa.

Peak 37 was identified as aloinoside A and/or B (stereoisomers of aloin-11-*α*-rhamnoside). This was noted at Rt 1018.4 s with a deprotonated mass peak at *m*/*z* 563.2. This compound was observed in *A. vera*, *A. arborescens*, *A. eru*, *A. grandidentata* and *A. perfoliata*.

Table 1
Peak assignments of metabolites identified in LC/MS spectrum of eight different *Aloe* species.

No.	Rt (s)	$[M-H]^-$	MS^n ion m/z (−) ppm	Tentative identification	A_1	A_2	A_3	A_4	A_5	A_6	A_7	A_8
1.	118.2	651	591, 501, 436, 349, 302, 206/489, 325, 205, 163, 119	*cis-p*-Coumaric acid derivatives	+	+	–	–	–	+	+	+
2.	248	515	464, 382, 301	3,4-di-*O*-(*E*)-Caffeoylquinic acid	–	–	–	–	–	–	+	–
3.	599	393	376, 304, 274, 245, 219, 203, 163	Aloesin (aloeresin B)	–	–	–	+	+	–	–	–
4.	603	439	380, 313, 274, 135	Unk	–	+	–	–	+	–	–	–
5.	672	593	431, 258, 175	Aloe emodin-diglucoside	–	+	–	+	–	–	–	+
6.	677	456	394, 364, 333, 291, 223	Unk	–	–	–	+	+	–	–	–
7.	698	395	350, 274.8, 230, 202/313, 259, 213	1-Hexanol-pentosylhexoside	–	–	–	–	+	–	–	–
8.	716	408	315, 252, 147/354, 303, 269, 233	Caffeoyl ferulic acid derivatives	–	–	–	+	–	–	–	–
9.	727	475	405, 301, 367, 286, 224, 145	Chrysoeriol-7-*O*-glycuronyl	–	–	–	+	–	–	–	–
10.	728	353	248, 209, 191, 179, 173, 161, 135, 145	5-*O*-caffeolyquinic acid	–	–	–	–	–	+	–	–
11.	796	601	563, 537, 529, 496, 429	Malonyl-*3,4-O*-dicaffeoyl quinic acid	+	–	–	–	–	–	+	–
12.	811.8	609	590, 518, 489	Luteolin-*6,8-C*-diglucoside (Lucenin II)	+	+	–	+	–	–	+	+
13.	841.9	595	533.1, 433, 415.6, 294.4, 314, 271, 145.1	6′-*O*-Caffeoyl-5-hydroxyaloin A	+	+	–	+	–	–	–	–
14.	857.8	542	145.4, 191.8, 250.0, 300.5, 360.9, 415.1, 505, 396	Unk	+	–	–	–	–	–	–	+
15.	871.2	593	575, 503, 473, 449, 383, 353, 287	Apigenin-6,8-*C*-diglucoside (vicenin II)	+	+	+	+	–	+	–	+
16.	875.2	620	583.0, 437.0, 370.8	*trans-p*-Coumaric derivatives	+	+	–	–	–	–	–	–
17.	888	529	475, 367, 192, 145	3-*O*-(*E*)-caffeoyl-4-*O*-feruloylquinic acid	–	+	+	+	+	–	–	–
18.	915.2	667	605, 513, 439, 394, 285, 232	Luteolin-*O*-xylosylglucoside malonylated	+	+	–	+	+	+	+	–
19.	915.8	702	541, 395, 233	Aloeresin C (isomer)	+	+	–	–	+	+	–	–
20.	921	739	704, 587, 577, 550, 453, 310, 289, 242	*Epi*-catechin digalloyl rhamnoside	–	–	–	–	+	+	–	–
21.	923.9	624	584.2, 517.0, 314	Isorhamnetin-*3-O*-deoxyhexosyl(1-6) hexoside	+	+	–	+	–	+	+	–
22.	934.8	581	516.2	7-*O*-Methyl kaempferol dimmer	+	+	–	–	+	–	–	–
23.	942.1	516	483.9, 354.9, 210.7, 186.7	Caffeoyl quinic acid hexoside	+	+	–	–	–	+	–	–
24.	945	411	246.8/249, 161, 113	Iso pentyldihexose	–	–	+	–	–	–	–	–
25.	948	445	439.6, 409, 248.8, 271, 269, 153	Apigenin-7-*O*-glycuronyl	–	–	+	–	–	–	–	–
26.	948.2	579	495.1, 447.4, 356.9, 287, 285	Kaempferol-*3*-*O*-hexosyl-*O*-pentoside	–	+		+	–	–	–	–
27.	948.2	447	357.3/405, 327, 147	Luteolin-*8-C*-glucoside (orientin)	+	+	–	+	+	–	–	+
28.	955.6	447.8	429.8, 405, 356.9, 326.9, 271, 147	Luteolin-*6-C*-glucoside (isoorientin)	+	–	–	+	–	–	–	–
29.	962.6	409.1	247	Aloenin	–	–	+	–	–	–	–	–
30.	970.2	499	472.0, 436.7, 312.5	3-*O*-Caffeoyl-*5*-*O*-coumaroylquinic acid	+	+	–	–	+	–	–	–
31.	976	613	570, 508, 457, 391	*4*-Succinyl-*3,4*-dicaffeoylquinic acid	–	+	–	–	+	+	+	–
32.	998	469	435/395, 298, 192, 149	Unk	–	–	–	+	–	–	–	+
33.	998	433	396.6, 342.9, 313, 269.8, 271, 255	5-Hydroxyaloin A	–	–	–	+	+	–	–	–
34.	1011.9	505	448, 343.1, 342.9, 341.1, 172	6′-Malonylnataloin (nataloin)	+	+	+	+	–	+	–	+
35.	1013.1	343	316, 315, 299, 287, 285, 236	5,3′-Dihydroxy-6,7,4′-trimethoxy flavones (Eupatorin)	–	+	+	+	–	+	–	–
36.	1018.1	463	515.8, 472.5/301	Isoquercetrin	–	+	+	–	–	–	–	–
37.	1018.4	563.2	505.5, 500, 435, 406, 342.9, 328, 290	Aloinoside A/B	+	+	+	+	+	–	–	–
38.	1025	483	446, 422, 325.9/337, 319, 173, 163	3,4-Di-*O*-(*E*)-*p*-coumaroylquinic acid	–	+	–	+	–	–	–	–
39.	1057	577	451, 425, 413, 305, 271, 293.4	*Epi* (afzelechin) – (*epi*) gallocatechin	–	–	+	+	+	–	–	–
40.	1063	543	500, 462, 361	Unk	+	+	–	+	–	–	–	–
41.	1081	509	492.6, 387.9, 345.9, 283.8, 212.9	Unk	+	+	–	–	–	–	–	–
42.	1084.2	506	396.5, 343.0, 342.9	Unk	+	+	–	–	–	–	–	–
43.	1096	570	548, 510.8, 471.9, 433, 411, 357.5, 320, 248, 203	2′-*O*-Feruloylaloesin	–	+	+	+	–	+	+	–
44.	1114	778	658, 570, 508, 455	Unk	–	–	–	+	+	–	–	–
45.	1120.5	616	582.7, 578.8, 516.8, 500.1, 393.2, 147.1, 145.3	7-*O*-Methylaloesin-penta acetate	+	+	–	–	+	–	+	–
46.	1121	583	570, 554, 477, 407, 243, 272	7-Methylether of 2′-feruloylaloesin	–	–	+	+	–	–	+	–
47.	1143.7	604	567.1, 500.3, 421.0	malonyl-4,5-*O*-dicaffeoylquinic acid	+	+	–	–	–	–	–	–

Table 1 (*Continued*)

No.	Rt (s)	[M−H]⁻	MS^n ion m/z (−) ppm	Tentative identification	A_1	A_2	A_3	A_4	A_5	A_6	A_7	A_8
48.	1161	629	547, 481, 208, 146/537, 425, 378, 325, 236, 178, 146	Glucuronides	–	–	+	–	+	–	–	–
49.	1164	670	616, 550, 473, 274	Unk	–	–	–	–	–	–	+	+
50.	1167	555	538, 512, 410, 392, 366, 259, 193, 147, 119	Isoaloeresin D	–	–	+	+	+	+	–	–
51.	1198	554	–	Unk	–	–	–	+	+	–	–	–
52.	1224.4	556	494, 423, 282, 207	Aloeresin	–	–	+	+	–	+	–	–
53.	1226	671	615, 581, 481	Unk	–	–	–	+	–	–	–	+
54.	1256.4	418	417.6, 343.2	Nataloin	+	+	–	+	–	–	–	–
55.	1258	297	–	Veracylglucan A	–	+	–	–	–	–	–	–
56.	1265	885	431, 307, 284	Kaempferol di deoxyhexosylhexoside	–	–	+	–	–	–	–	+
57.	1281.6	833	636.2, 713.5, 775.6	Unk	+	+	–	+	–	–	–	–
58.	1290	713	635.9, 564.3, 516.5, 343.4	Aloenin B	+	+	+	+	–	–	–	–
59.	1292.0	747	482.1	Wighteone-*O*-diglucoside malonylate	+	+	–	–	–	–	–	–
60.	1302.1	417	396.1, 343.1, 296.9	Aloin A	+	+	–	+	–	–	–	–
61.	1318	417	145, 297, 343	Aloin B	+	–	–	+	–	–	–	–
62.	1328	432	361, 359, 353, 340.7, 310, 283, 269	Isovitexin (6-*C*-glucosyl-apigenin)	–	–	–	–	+	–	–	–
63.	1342	539	432, 359, 312, 254, 146	6′-*O*-Coumaroyl aloesin	–	–	–	–	+	–	–	–
64.	1366	297	248.9, 174.9	Hydroxy octadecenic acid	–	–	–	+	–	–	–	–
65.	1396	586.9	587, 518.1, 427, 257, 147	Unk	–	–	+	–	–	–	–	–
66.	1407	540	468, 420, 393, 312	Aloeresin A isomer	–	–	–	–	+	–	–	–
67.	1410	329.7	286, 214, 147	Trihydroxy octadecenoic acid	–	–	–	–	–	–	+	–
68.	1424	1016	979, 916.9, 859.6, 834.9, 606, 144.8	Unk	+	+	–	–	–	+	–	–
69.	1430	657.6	620, 530, 458/533, 480, 391, 134	Unk	–	–	–	+	+	–	–	–
70.	1448	869.2	833, 717, 650, 586.3, 511.3, 144.7	Unk	+	+	–	+	–	–	–	–
71.	1460	569	426, 355, 285, 225, 161	Caffeoylester of aloesin	–	+	+	–	+	–	–	–
72.	1462	496	418, 225, 397, 285, 248, 145	Unk	–	+	+	–	–	–	–	–
73.	1507	580	463, 326, 296, 265	Unk	–	–	–	+	–	+	–	–
74.	1519	605	562, 425, 317, 267, 146, 92	Unk	–	–	+	–	–	+	–	–
75.	1590	565	534, 488, 343, 241	Trihydroxycinnamic acid derivatives	–	–	–	+	–	–	–	–
76.	1600	599	564, 512, 443.0	Unk	+	+	–	+	–	–	–	–
77.	1611	685	623, 571, 500, 523.3, 539, 521	Aloeresin E	+	+	+	+	+	-	-	+
78.	1612	557	505, 444, 392, 322, 251	Acetyl dicaffeoylquinic acid	–	–	–	+	+	–	–	–
79.	1645	831.3	813.2, 711.2, 669.8, 742, 686, 553	Unk	+	+	–	–	–	–	–	+
80.	1659.9	416.4	267.8	Barbaloin (10*R*)/Isobarbaloin (10*S*)	+	+	–	–	–	–	–	–
81.	1666	445	380, 295, 256, 216, 145/269	Apigenin-7-*O*-glycuronyl	–	–	+	–	–	–	–	–
82.	1725	741.6	416, 301, 300/609, 301	Quercetin pentosyl rutinoside	–	–	–	–	–	–	–	+
83.	2083	689.1	854, 603, 505	Unk	–	+	–	–	+	+	–	–
84.	2097	675.9	640, 586, 534/640, 506, 497	Unk	–	–	–	–	+	+	+	–
85.	2117.8	711.9	675.2, 550.6, 396.9	Quercetin-7-*O*-hexoside-3-*O*-malonylhexoside	+	+	–	–	+	–	+	–
86.	2174	431	316.1, 269, 225	Aloe-emodin-8-*O*-glucoside	+	+	+	–	+	–	+	+
87.	2226	553	408, 376, 341, 275, 259, 256, 233, 193, 178, 161	2′-*p*-Methoxycoumaroylaloresin	–	–	+	–	+	–	+	–
88.	2235	552	448.1, 359.8, 145.1	Unk	–	+	–	–	+	–	–	–
89.	2252	715	625.6, 553.6, 455.1, 357.6, 303.8, 207, 129.2	Unk	–	+	–	–	–	–	–	–
90.	2293	567	528, 313, 271, 253, 169	Chrysophanol-*8*-*O*-(*6′*-*O*-galloyl-) glucoside	–	+	–	–	–	–	–	+
91.	2339	637	579, 504, 359	Unk	–	–	–	–	–	–	+	–
92.	2450	825	788, 669, 626, 581, 514, 452, 394	Aloeresin H tetra-*O*-methyl ether	–	–	–	–	–	–	+	–
93.	2549	769	730.5, 326.1	Aloeresin H	–	+	–	–	+	–	–	–
94.	2574	612	555, 492.3, 427, 260.4	Unk	+	+	+	–	+	–	–	–
95.	2603	642, 643	612, 557, 513, 446, 375, 269, 135/550, 501/580, 508, 459	Unk	–	–	+	–	+	–	+	+
96.	2625	809.8	642, 556, 515, 448	Unk	+	+	–	–	+	–	+	–
97.	2632	444.2	392, 203.7	Unk	+	+	–	–	–	–	–	–
98.	2650	811.8	777.8, 672.4, 573.3, 512.8, 462.3, 392, 341, 269, 135	Unk	–	+	–	–	+	–	–	–
99.	2712	813.4	529.4, 462.4	Unk	–	+	–	–	+	–	–	–
100.	2768	789.6	672.3, 612.6, 533.9, 467, 398.7, 308.8, 272, 135, 93	Unk	–	+	–	–	–	–	–	–
101.	2871	627.8	571.2, 505.8, 444.8, 388.7, 135.6/481, 319	Pentahydroxyflavonol-*O*-hexosyl rhamnoside	–	+	–	–	+	–	–	–
102.	2872	532/533	464, 388, 171/489, 285	Kaempferol-3-*O*-malonylhexoside	–	–	–	+	+	–	–	–

A_1 = *Aloe vera*, A_2 = *A. arborences*, A_3 = *A. eru*, A_4 = *A. grandidentata*, A_5 = *A. perfoliata*, A_6 = *A. brevifolia*, A_7 = *A. saponaria*, A_8 = *A. ferox*. Unk = unknown.
(+) denotes presence and (−) denotes absence of each compound in examined *Aloe* species

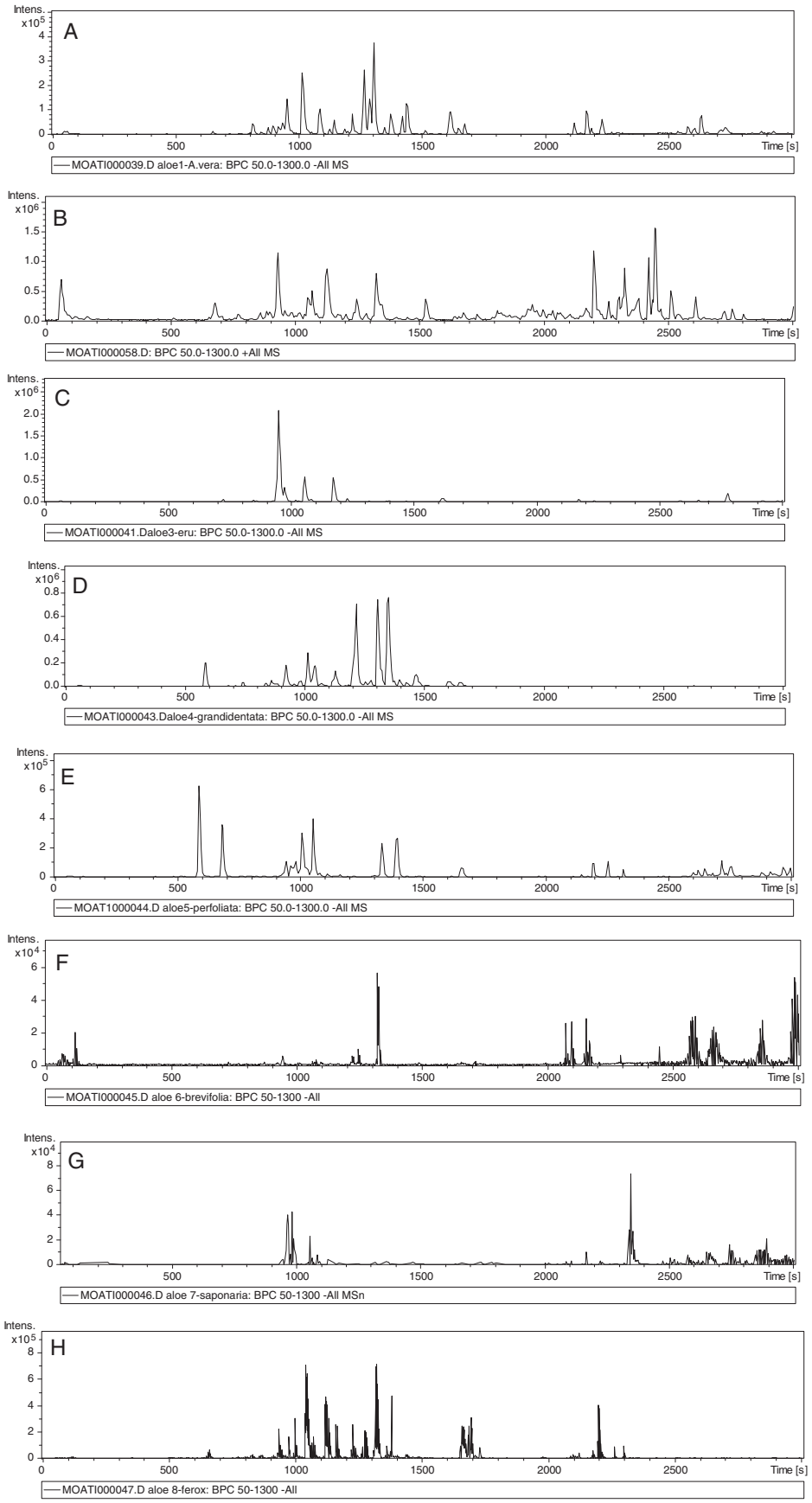

Fig. 1. HPLC fingerprint of **A**, *Aloe vera*; **B**, *A. arborences*; **C**, *A. eru*, **D**, *A. grandidentata*; **E**, *A. perfoliata*; **F**, *A. brevifolia*; **G**, *A. saponaria*, **H**, *A. ferox* recorded at 254 nm.

ESI-MS spectrum of peak 45 (Rt 1120.5 s) showed $[M-H]^-$ at *m/z* 616 which on further fragmentation yielded ions at *m/z* 516, 500, 393 and 147. This compound was identified as 7-*O*-methylaloesin penta acetate and detected in *A. vera*, *A. arborescens*, *A. perfoliata* and *A. saponaria*.

The negative ESI-MS of peak 46 (Rt 1121 s) showed strong peaks at *m/z* 583 $[M-H]^-$ which yielded a peak at *m/z* 407 $[M-177]^-$ due to the loss of a fragment with mass 177. This could be interpreted as the loss of a (COCH=CHC_6H_3 (OCH_3) OH) fragment from a ferulic acid derivative. This fragmentation is followed by the loss of water from *m/z* 407. The spectrum showed no peaks corresponding to the subsequent loss of the carbohydrate moiety after the loss of the acyl group. In contrast, the negative ESI-MS of aloesin showed a strong $[M-H]^-$ ion and a base peak at *m/z* 272 corresponding to the loss of carbohydrate moiety. This compound was identified as (*E*)-2-acetonyl-8-(2′-*O*-feruloyl)-β-D-glucopyranosyl-7-methoxy-5-methylchromone (**11**, 7-methylether of 2′-feruloylaloesin) and detected in *A. eru*, *A. grandidentata* and *A. saponaria*. 7-Methylether of 2′-feruloylaloesin was previously reported in the leaves of *A. broomii*, *A. Africana* and *A. speciosa* (Holzapfel et al., 1997).

Peak 50 (Rt 1167 s) revealed a molecular ion peak at *m/z* 555 $[M-H]^-$, consistent with a molecular weight 556 which was detected in *A. eru*, *A. grandidentata*, *A. perfoliata* and *A. brevifolia*. MS/MS analysis revealed the following fragments at *m/z* 538 $[M-H_2O]$ ($[M-18]^-$), *m/z* 512 $[M-CH_3CHO]$ ($[M-44]^-$), *m/z* 410 [M–coumaroyl] ($[M-146]^-$), *m/z* 392 $[M-(146+18)]^-$, *m/z* 366 $[M-(146+44)]^-$, *m/z* 259 $[M-(133+146+18)]^-$, *m/z* 193$[M-(133+146+84)^-]$, *m/z* 147 $[coumaroyl]^+$ and *m/z* 119 $[HOC_6H_4CHCH]^+$. This spectra was consistent with the spectrum reported by Lee et al. (2000) for isoaloeresin D (**12**, 8-*C*-β-D-[2-*O*-(*E*)-coumaroyl]glucopyranosyl-2-[2-hydroxy]-propyl-7-methoxy-5-methyl chromone).

Nataloin was detected as peak 54 (Rt 1256.4 s) with $[M-H]^-$, at *m/z* 418, this compound was observed in *A. vera*, *A. arborescens* and *A. grandidentata*. Aloin A/B (**13**, 10-*C*-β-D-glycopyranoside of aloe-emodin-anthrone), which in most cases was detected as a mixture of α- and β-stereoisomers (MW 418), was previously isolated from the leaf exudates of the non maculate Kenyan species (Conner et al., 1987). Aloin A was observed in the leaf extract of *A. vera*, *A. arborescens*, and *A. grandidentata* as peak 60 with $[M-H]^-$ at *m/z* 417. Peak 61 (Rt 1318 s) which showed $[M-H]^-$ at *m/z* 417 was identified as aloin B and was detected in *A. vera* and *A. grandidentata*.

Peak 63 (Rt 1342 s) was identified as a chromone; 6-*O*-coumaroyl aloesin having $[M-H]^-$ at *m/z* 539 which was detected only in *A. perfoliata*. This chromone is a marker metabolite restricted to the section *Anguialoe*, thus providing chemotaxonomic corroboration for the presumed monophyly of the section (All species of *Aloe* that belong to section *Anguialoe* share a single, unique apomorphy which is the sessile flowers) (Reynolds, 1985).

Peak 66 (Rt 1407 s) with $[M-H]^-$ at *m/z* 540 consistent with a molecular weight 541 of aloeresin A (**6**). The daughter fragment at *m/z* 393 with difference 146 amu was in agreement with the loss of a *p*-coumaroyl group. In previous work dealing with the mass spectral characterization of plant glycoconjugates, a neutral loss of 120 amu due to a cross-ring cleavage in the hexosidic part for deprotonated and protonated flavonoids *C*-glycosides was reported (Wang et al., 2003). The latter loss has also been reported for the protonated chromone *C*-glycosides, aloesin and aloeresin A. Aloeresin A was detected only in *A. perfoliata*.

Mass spectra of peak 71 at (Rt 1460 s) showed $[M-H]^-$ at *m/z* 569 which was tentatively interpreted as caffeoyl ester of aloesin. The compound was identified as (*E*)-2-acetonyl-8-(2′-*O*-caffeoyl)-β-D-glucopyranosyl-7-methoxy-5-methyl chromone and observed in *A. arborescens*, *A. eru* and *A. perfoliata*. Peak 77 (Rt 1611 s) showed $[M-H]^-$ at *m/z* 685 which was tentatively interpreted as (*E*)-2-acetonyl-(2′,6′-di-*O*,*O*-coumaroyl)-β-D-glucopyranosyl-7-hydroxy-5-methyl chromone (aloeresin E, **14**). This compound was observed in *A. vera*, *A. arborescens*, *A. eru*, *A. grandidentata*, *A. perfoliata* and *A. ferox*. MS^2 showed daughter fragment ions at *m/z* 539 and 521 corresponded to the loss of acetonyl and coumaroyl plus carbohydrate moieties from the parent molecules, respectively. Mass spectrum of peak 86 (Rt 2174 s) showed $[M-H]^-$ at *m/z* 431 which was tentatively interpreted as aloe-emodin-8-*O*-glucoside (**14**). MS^2 of the compound showed fragment ions at *m/z* 316, 269, and 225. This was detected in *A. vera*, *A. arborescens*, *A. eru*, *A. perfoliata*, *A. saponaria* and *A. ferox*.

Peak 87 (Rt 2226 s) in the negative ion mode showed a deprotonated parent ion peak at *m/z* 553 $[M-H]^-$. A daughter ion was obtained in MS^2 due to loss of *p*-methoxy coumaric acid at *m/z* 376 and the presence of the *p*-methoxy coumaroyl fragment ion at *m/z* 161 which were consistent with the previously reported data for 2′-*p*-methoxy coumaroylaloeresin in leaves of *A. excels* (Mebe, 1987). This compound was detected in *A. eru*, *A. perfoliata* and *A. saponaria*.

The ESI-MS spectrum of peak 92 (Rt 2450 s) gave deprotonated molecule $[M-H]^-$ at *m/z* 825 which was tentatively interpreted as aloeresin H tetra-*O*-methylether observed only in *A. saponaria*. For peak 93 (Rt 2549 s), the ESI-MS spectrum gave deprotonated molecule $[M-H]^-$ at *m/z* 769 which was tentatively interpreted as aloeresin H (*C*,*C*-di-glucoside polyketides) and observed only in *A. arborescens* and *A. perfoliata*.

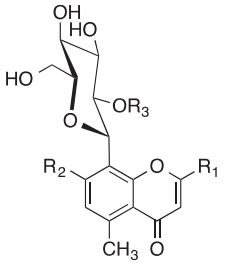

4 R_1=CH_2COCH_3; R_2=OH; R_3=H
5 R_1=CH_2COCH_3; R_2=β-D-Glc; R_3=*p*-(*E*)-coumaroyil
6 R_1=CH_2COCH_3; R_2=OH; R_3=*p*-(*E*)-coumaroyil
11 R_1=CH_2COCH_3; R_2=OCH_3; R_3=feryolyl
12 R_1=$CH_2CH(OH)CH_3$; R_2=OCH_3; R_3= *p*-(*E*)-coumaroyil
14 R_1=CH_2COCH_3; R_2=β-D-Glc; R_3=cinnamoyl

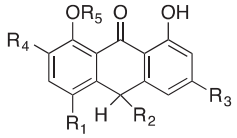

9 R_1=OH; R_2=β-D-Glc; R_3=CH_2OH; R_4=R_5=H
10 R_1=R_5=H; R_2=6'malonylglucose; R_3=CH_3; R_4=OH
13 R_1=R_4=R_5=H; R_2=β-D-Glc R_3=CH_2OH

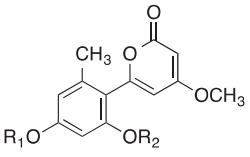

7 R_1=H; R_2=glucopyanoxyl
8 R_1=β-D-glucosyl; R_2=*p*-*E*-coumaroylglucosyl

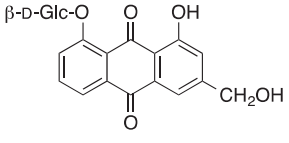

14

C-glycosylflavonoids

The occurrence of flavonoids such as isoorientin (**15**, luteolin-6-*C*-glucoside) and isovitexin (**16**, apigenin 6-*C*-glucoside) was observed in biogeographical trends. Isoorientin is a common constituent of tropical and sub-tropical species of *Aloe*, whereas isovitexin is restricted to a few southern African species. Isoorientin and isovitexin co occur in the Southern African maculate species; *A. parvibracteata*, and the disjunct West African maculate species, *A. macrocarpa*. The presence of isoorientin and isovitexin in maculate species of *Aloe* was first reported by Grace *et al.*, 2010. The presence of flavonoids in section *Pictae* is therefore of taxonomic interest.

ESI-MS spectrum of Peak 12 (Rt 811.8 s) showed $[M-H]^-$ at *m/z* 609, its MS/MS spectrum give rise to daughter ions at *m/z* 590 $[(M-H)-18]^-$, 518 $[(M-H)-90]^-$ and a base peak at *m/z* 489 $[(M-H)-120]^-$. This compound was tentatively characterized as luteolin-6,8-*C*-diglycoside (**17**, lucenin II). The MS/MS spectrum of peak 15 (Rt 871.2 s) in negative ion mode with $[M-H]^-$ at *m/z* 593 which produced daughter ions at *m/z* 575 $[(M-H)-18]^-$, *m/z* 503 $[(M-H)-90]^-$ and a base peak at *m/z* 473 $[M-H-120]^-$, exhibiting a fragmentation pattern of flavones di-*C*-glycoside. The ions at *m/z* 353 $[(M-H)-(120+120)]^-$ and at *m/z* 383 $[(M-H)-(90+120)]^-$ indicated the presence of apigenin (MW 270) as aglycone and two hexose moieties (glucoses). Comparing with MS literature data (Piccinelli *et al.*, 2008), this compound was characterized as 6,8-di-*C*-glucosylapigenin and also known as vicenin II (**18**).

Peak 27 (Rt 948.2 s), showed ESI-MS spectrum with $[M-H]^-$ at *m/z* 447. Tendam mass of this peak yielded fragment ions at *m/z* 357.3 $[(M-H)-90]^-$ and a base peak at 327 $[(M-H)-120]^-$, together with the absence of the loss of 18 amu suggesting that the mono-*C*-glycosylation is in position 8 (Ferreres et al., 2007). Peak 27 was tentatively characterized as luteolin 8-*C*-glucoside, also known as orientin (**19**). This compound was detected in *A. vera*, *A. arborescens*, *A. grandidentata*, *A. perfoliata* and *A. ferox*. ESI-MS spectrum of peak 28 (Rt 955.6 s) showed a deprotonated molecule $[M-H]^-$ at *m/z* 447.8. The spectrum exhibited fragments at *m/z* 356.9 $[(M-H)-90]^-$ and a base peak at 326.9 $[(M-H)-120]^-$. For flavones mono-*C*-hexosides, the position of the sugar residue can be assigned through observation of the abundance of fragment ion [(M−H)-18]. In general, the fragmentation of the 6-*C*-isomers is more extensive, giving an ion corresponding to *m/z* 429 $[(M-H)-18]^-$, probably due to the formation of an additional hydrogen bond between the 2″-hydroxyl group of the sugar and the 5- or 7-hydroxylgroup of the aglycone, which confers additional rigidity (Abad-Garcia et al., 2009). The abundance of fragment ion at 429.8 suggested the mono-*C*-glycosylation is in position 6, hence, compound 28 was identified as luteolin-*6*-*C*-glucoside, also known as isoorientin (**15**). Isoorientin was detected in *A. vera* and *A. grandidentata*.

Peak 62 at Rt 1328 s, in which the ESI-MS spectrum showed $[M-H]^-$ at *m/z* 432 was characterized as *6*-*C*-glycosyl apigenin, also known as isovitexin (**16**). Its MS/MS spectrum gave mass fragmentation at *m/z* 340.7 and 310. Isovitexin was observed only in *A. perfoliata*. The main product ions in the negative ionization mode were due to dehydration, cleavage of sugar ring, and the loss of glycosidic methyl group as formaldehyde. In addition, the intensity ratios of these major fragments could be a way to differentiate vitexin from isovitexin (Abad-García et al., 2008). The MS/MS in the negative ionization mode, the product ions obtained with cleavage of sugar ring was proposed as diagnostic ions, since *m/z* 313 is the base peak of apigenin-8-*C*-glycoside and *m/z* 283 is the base peak of apigenin-6-*C*-glycoside. In contrast, an ion at *m/z* 361 was only found in apigenin-*6*-*C*-glycoside, probably because of the additional hydrogen bond that is required for loss of the extra water (Abad-García et al., 2008).

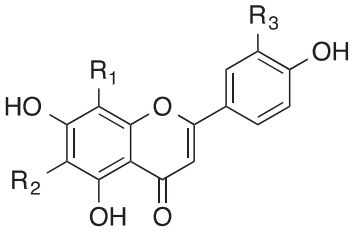

15 R_1=H; R_2=β-D-Glc;R_3=OH
16 R_1=R_3=H; R_2=β-D-Glc
17 R_1=R_2=β-D-Glc; R_3=OH
18 R_1=R_2=β-D-Glc; R_3=H
19 R_1=β-D-Glc; R_2=H; R_3=OH

O-Glycosylflavonoids

Peak 9 showed precursor ions at *m/z* 475 $[M-H]^-$ and MS^2 at *m/z* 301, corresponding to the loss of a glycuronyl unit. A further fragmentation of the precursor ion at *m/z* 301 resulted in a product ion at *m/z* 286, produced by the loss of methyl group (El-Hela et al., 2010). Therefore, peak 9 was identified as chrysoeriol-7-*O*-glycuronyl detected only in *A. grandidentata*.

MS spectra interpretation allowed the assignment of the compound luteolin-*O*-xylosylglucoside malonylated as peak 18 and its molecular ion at *m/z* 667 and further fragmentation of parent ion which gave aglycone fragment at *m/z* 285 as the most abundant ion in the fragmentation spectrum (Wojakowska et al., 2013) indicating the presence of luteolin. Malonylation increase both the affinity and transportation, of anthocyanins or other flavonoids and facilitate their transport into the vacuole by a defined transporter. It has been suggested that aromatic acylation enhances the color of anthocyanins, whereas aliphatic acylation (usually malonylation) may stabilize flavonoids and increase the resistance of flavonoid glucoside malonates to enzymatic degradation (Luo et al., 2007). Malonylation of flavonoids occurs widely in plants, and malonyltransferases have been characterized from several different species (Yu et al., 2008). Malonylation, but not *p*-coumaroylation, of flavonoids induces a conformational change that might facilitate their transport and storage in the vacuole, possibly through improved solubility and reaction with other vacuolar components (Matern et al., 1983). Compound 18 was observed in all of the investigated *Aloe* species except *A. eru* and *A. ferox*. The presence of flavonoids in section *Pictae* is of taxonomic interest.

Peak 21 (Rt 923.9 s) was identified as isorhamnetin derivative. Isorhamnetin is a methylated derivative of quercetin and it was identified on the basis of the presence of a specific base peak at *m/z* 314, in addition to characteristic loss of a methyl from its methoxy group (−15 amu). The results were consistent with the loss of a deoxyhexosyl-hexoside moiety (308 amu). Compound 21 was identified as isorhamnetin-3-*O*-deoxyhexosyl-(1-6) hexoside and was noted in *A. vera*, *A. arborescens*, *A. grandidentata*, *A. brevifolia* and *A. saponaria*.

The mass spectrum of peak 25 at (Rt 948 s) showed precursor ion in the negative ionization mode at *m/z* 445 $[M-H]^-$ and a daughter ion peak at *m/z* 269, corresponding to the loss of a glycuronyl unit. Therefore, this compound was identified as apigenin-7-*O*-glycuronyl (Surowiec et al., 2007; Petroviciu et al., 2010) noted only in *A. eru*.

Mass spectrum of peak 26 (Rt 948.2 s) showed precursor ions at *m/z* 579 $[M-H]^-$ could be identified as a kaempferol-hexosyl-pentoside based on the fragment at *m/z* 447 $[(M-H)-132]^-$ and at *m/z* 285 $[(M-H)-132-162]^-$. Therefore, peak 26 was identified as kaempferol-3-*O*-hexosyl-pentoside. It is important to note that product ion at *m/z* 287 showed a fragmentation pattern in

Table 2
Anti-inflammatory activity of the methanol extract of the eight *Aloe* species (A_1–A_8).

Time (h)	Zero	1 h		2 h		3 h		4 h	
Group	Paw diameter (mm)	Paw diameter (mm)	Edema thickness (mm)	Edema thickness (mm)	Paw diameter (mm)	Edema thickness (mm)	Paw diameter (mm)	Paw diameter (mm)	Edema thickness (mm)
Control	3.30 ± 0.08	4.41 ± 0.1[a]	1.11	4.71 ± 0.13[a]	1.41	4.81 ± 0.12[a]	1.51	4.85 ± 0.07[a]	1.55
A. vera	3.33 ± 0.08	4.26 ± 0.10[a]	0.93	4.10 ± 0.13[a]	0.77	3.82 ± 0.12[a]	0.49	3.64 ± 0.08[a]	0.31
A. arborences	3.49 ± 0.09	4.34 ± 0.09[a]	0.85	4.21 ± 0.08[a]	0.72	4.03 ± 0.09[a]	0.55	3.84 ± 0.09[a]	0.35
A. eru	3.51 ± 0.10	4.38 ± 0.14[a]	0.87	4.28 ± 0.14[a]	0.77	4.12 ± 0.14[a]	0. 61	3.94 ± 0.11[a]	0.43
A. grandidentata	3.56 ± 0.11	4.16 ± 0.20[a]	0.6	3.99 ± 0.10[a]	0.43	3.95 ± 0.05[a]	0.39	3.90 ± 0.7[a]	0.34
A. perfoliata	3.57 ± 0.1	4.46 ± 0.12[a]	0.89	4.27 ± 0.14[a]	0.70	4.04 ± 0.05[a]	0.47	3.94 ± 0.05[a]	0.37
A. brevifolia	3.49 ± 0.06	4.37 ± 09[a]	0.89	4.30 ± 0.06[a]	0.81	4.27 ± 0.07[a]	0.78	4.03 ± 0.6[a]	0.54
A. saponaria	3.61 ± 0.02	4.51 ± 0.07[a]	0.90	4.38 ± 0.02[a]	0.87	4.14 ± 0.08[a]	0.53	4.08 ± 0.06[a]	0.47
A. ferox	3.60 ± 0.09	4.49 ± 0.09[a]	0.89	4.31 ± 0.08[a]	0.71	4.11 ± 0.09[a]	0.51	3.98 ± 0.09[a]	0.38
Indomethacin	3.56 ± 0.08	4.12 ± 0.09[a]	0.6	3.99 ± 0.06[a]	0.43	3.92 ± 0.01[a]	0.36	3.84 ± 0.07[a]	0.28

[a] Significantly different from zero time at $p < 0.05$ ($n = 6$).
The dose of the extracts was 250 mg/kg.

agreement to kaempferol (Cuyckens and Claeys, 2004; Vallverdú-Queralt et al., 2010).

Mass spectrum of peak 35 (Rt 1013.1 s) showed $[M-H]^-$ at m/z 343, it was identified as dihydroxyl trimethoxyflavone (5,3′-dihydroxy-6,7,4′-trimethoxyflavone) Eupatorin and noted in *A. arborescens*, *A. eru*, *A. grandidentata* and *A. brevifolia*. MS/MS spectrum gave product ions at m/z 316, 315, 299 and 287, which were in accordance to this compound (Jaffer and Mahmoud, 2011; Akowuah et al., 2012).

Peak 36 (Rt 1018.1 s) showed $[M-H]^-$ at m/z 463 consistent with the molecular formula ($C_{21}H_{20}O_{12}$). MS/MS spectrum of this compound showed a product ion at m/z 301 indicating a quercetin nucleus (Breiter et al., 2011). This peak was compared with authentic standard and identified as quercetin-3-*O*-glucoside (isoquercetrin) and was noted only in *A. arborensis* and *A. eru*.

HPLC analysis of the methanol extract of the leaves of the eight investigated *Aloe* species revealed apart from the known metabolites; aloesin (**4**), nataloin (**10**), aloin A/B (**13**), aloeresin E (**14**) and aloeresin H, which are of particular importance in the chemotaxonomic study of the genus *Aloe*. Barbaloin/isobarbaloin, which is *C*-glucoside of aloe emodin anthrone (10-β-D-glucopyranosyl-1,8-dihydroxy-3-hydroxymethyl-9 (10H)-anthracenone) are considered to be the most specific secondary phytoconstituent in *Aloe* species. Barbaloin has been found to have a strong inhibitory effect on histamine release from mast cells (Patel et al., 2012). Aloeresin H, 8-*C*-β-D-glucopyranosyl-7-hydroxy-5-methylchromone portion that is common to all aloeresins (A–G) were detected in most of the investigated *Aloe* species. Aloeresin Hrepresents the first *C*,*C*-diglucosylated molecule discovered in *Aloe* spp. extracts. Although cinnamic acid derivatives are present in *Aloe* metabolites in the aloin series, aloeresin E (**14**) and aloeresin F represent the first cinnamic acid derivatives in the aloeresin series of metabolites (Van Heerden et al., 1996). Aloenin B (**8**), a new bitter glycoside was detected in most of the leaves of the investigated *Aloe* species. 6′-Malonylnataloin (**10**), a malonylated derivative of the rare anthrone nataloin, also was identified in all investigated samples of *Aloe*. Anthrone *C*-glycosides are among a suite of chemical constituents of systematic importance in *Aloe*.

Aloe has long been recognized by different pharmacopeias over the world as a purgative drug (Rowson et al., 1967; Osol et al., 1973). The purgative effects of *Aloe* leaf (drug aloes) have been attributed to anthraquinone *C*-glycosides, notably barbaloin, aloin A and B (Steenkamp and Stewart, 2007). Further studies were conducted to investigate the Aloe's constituents responsible for this activity. Anthranol, aloe-emodin, chrysophanic acid (chrysophanol), aloin (barbaloin) and *p*-coumaric acid were previously reported in *A. vera*. A thin layer chromatographic study of 22 species of *Aloe* (Meredova et al., 1973) showed that twelve species contain flavonoids, hydroxy anthraquinones and coumarin.

Concerning the diabetic wound healing effect of the methanol extracts of the eight investigated *Aloe* species, results obtained in the present study suggested that treatment of diabetic rats with the methanol extract of each of the eight studied *Aloe* species may have a beneficial influence on wound healing. It is noteworthy to mention that the eight investigated species showed significant anti-inflammatory activity (Table 2) as their action in reducing the thickness of edema started from the first hour and continued for the four hours. The anti-inflammatory activity of *Aloe* may be due to the inhibition of the cyclooxygenase pathway and reduction of prostaglandin E2 production this could be attributed to its *C*-glucosyl chromones (Hutter et al., 1996). The findings of our study confirmed the significant acceleration of diabetic wound healing in rats following topical application of the methanolic extract of the leaves of the various *Aloe* species. The healing effect on the

Table 3
Effect of the methanol extract of the eight *Aloe* species on wound area in diabetic rats.

The tested sample	Wound area (cm^2)			
	Zero time	Day 2	Day 6	Day 10
Control	1.53 ± 0.003	1.55 ± 0.002	1.59 ± 0.001[a]	1.60 ± 0.003[a]
A. vera	1.58 ± 0.001	1.26 ± 0.004[a]	0.69 ± 0.003[a]	0.36 ± 0.001[a]
A. arborences	1.63 ± 0.002	1.23 ± 0.002[a]	0.67 ± 0.001[a]	0.46 ± 0.001[a]
A. eru	1.67 ± 0.002	0.89 ± 0.003[a]	0.46 ± 0.001[a]	0.23 ± 0.001[a]
A. grandidentata	1.71 ± 0.001	1.49 ± 0.002[a]	1.13 ± 0.002[a]	0.74 ± 0.001[a]
A. perfoliata	1.69 ± 0.003	1.41 ± 0.001[a]	0.86 ± 0.001[a]	0.53 ± 0.001[a]
A. brevifolia	1.56 ± 0.001	1.45 ± 0.001[a]	0.81 ± 0.002[a]	0.63 ± 0.002[a]
A. saponaria	1.68 ± 0.002	1.34 ± 0.002[a]	0.65 ± 0.001[a]	0.31 ± 0.001[a]
A. ferox	1.51 ± 0.001	1.37 ± 0.003[a]	0.98 ± 0.001[a]	0.47 ± 0.002[a]
Dermazine®	1.65 ± 0.004	0.72 ± 0.001[a]	0.43 ± 0.002[a]	0.13 ± 0.001[a]

[a] Significantly different from zero time at $p < 0.05$ ($n = 6$).

Table 4
Percent of change in wound area in diabetic rats treated with methanol extract of the eight *Aloe* species.

The tested samples	% of change in wound area		
	Day 2	Day 6	Day 10
Control	1.31	3.92	4.6
A. vera	30.30	56.3	77.2
A. arborences	24.5	58.8	71.8
A. eru	46.71	72.9	86.2
A. grandidentata	12.9	33.9	57.9
A. perfoliata	17.2	59.2	68.6
A. brevifolia	7.1	48.1	59.6
A. saponaria	20.2	61.3	81.6
A. ferox	14	35.1	68.9
Dermazine®	56.4	73.9	92.1

diabetic wounds was observed for the topical application of the methanol extracts of the eight studied *Aloe* species (Table 3), however, *A. eru* showed the highest effect in reducing the wounds area which reached 86.2% by day 10 (Table 4). It was previously reported that the healing properties of *Aloe* could be attributed to its glucomannan type polysaccharide, which stimulates the activity of fibroblasts and causes proliferation, which in turn increases collagen synthesis (Chithra et al., 1998). The high wound healing activity observed for *A. eru* could be mainly attributable to its major constituent aloenin, which was reported to significantly promote hair growth and demonstrated recuperative effects on human skin (Wolfson and Gutterman, 2009). Aloenin was detected only in *A. eru* (Table 1).

Conclusion

The occurrence of flavones-*C*-glycosides, heptaketides (*e.g.* 5-methylchromones) and octaketides (*e.g.* 1,8-dihydroxy-9-anthrones) in *Aloe* species is known. The results obtained here showed that these species possess different chemical composition, justifying the importance of studies aiming for the chemical characterization of different *Aloe* species. The anti inflammatory and wound healing activity of the *Aloe* species has been attributed to polyphenolic compounds. *A. eru* showed the highest effect in reducing the wounds area in ten days which is rich in Aloenin. Among the species presented in this paper, flavonoids are found as main constituents specially lucienin II, vicenin II, orientin and isovitexin in *A. vera*, *A. arborescens*, *A. grandidentata*, *A. perfoliata*, *A. brevifolia* and *A. saponaria*. Heptaketides (5-methylchromones) are found as main constituents in all investigated *Aloe* species except *A. vera*, *A. perfoliata* and *A. ferox*. Polyketides are of chemotaxonomic interest in all *Aloe* species investigated.

Ethical disclosures

Protection of human and animal subjects. The authors declare that the procedures followed were in accordance with the regulations of the relevant clinical research ethics committee and with those of the Code of Ethics of the World Medical Association (Declaration of Helsinki).

Confidentiality of data. The authors declare that no patient data appear in this article.

Right to privacy and informed consent. The authors declare that no patient data appear in this article.

Authors' contributions

AME contributed in collecting the plant material, preparation of some of the methanol extracts, interpretation of the HPLC–MS/MS data and constructing the manuscript. SME contributed in preparation of some of the methanol extracts, interpretation of the HPLC–MS/MS data, revising and finalizing the manuscript and interpretation of the biological results. MME contributed in performing the HPLC–MS/MS analysis and revising the interpretation of HPLC–MS/MS data. SSE contributed in suggesting the point of the research and supervising the work.

Conflicts of interest

The authors declare no conflicts of interest.

Acknowledgment

The authors are deeply thankful to Prof. Dr. Wafaa El Eraky, Department of Pharmacology, National Research Center, Giza, Egypt, for carrying out the biological experiments.

References

Abad-Garcia, B., Berrueta, L.A., Garmon-Lobato, S., Gallo, B., Vicenete, F., 2009. A general analytical strategy for the characterization of phenolic compounds in the fruit juices by high performance liquid chromatography with diode array detection coupled to electrospray ionization and triple quadraupole mass spectrometry. J. Chromatogr. A. 1216, 5398–5415.

Abad-García, B., Garmón-Lobato, S., Berrueta, L.A., Gallo, B., Vicente, F., 2008. New features on the fragmentation and differentiation of C-glycosidic flavone isomers by positive electrospray ionization and triple quadrupole mass spectrometry. Rapid Commun. Mass Spectrom. 22, 1834–1842.

Akowuah, G.A., Ismail, Z., Ahmed, M., 2012. HPLC-TOF/MS profile and nitric oxide scavenging activity of *Orthosiphon stamineus* leaf extracts. Asian Pac. J. Trop. Biomed., S1436–S1439.

Beppu, H., Nagamura, Y., Fujita, K., 1993. Hypoglycaemic and antidiabetic effects in mice of *Aloe arborescens* miller var. *natalensis* berger. Phytother. Res. 7, S37–S42.

Breiter, T., Laue, C., Kressel, G., Gröll, S., Engelhardt, U.H., Hahn, A., 2011. Bioavailability and antioxidant potential of rooibos flavonoids in humans following the consumption of different rooibos formulations. Food Chem. 128, 338–347.

Chithra, R., Sajithlal, G.B., Chandrakasan, G., 1998. Influence of *Aloe vera* on collagen characteristics in healing dermal wounds in rats. Mol. Cell Biochem. 181, 71–76.

Conner, J.M., Gray, A.I., Waterman, P.G., Reynolds, T., 1990. Novel anthrone-anthraquinone dimers from *Aloe elgonica*. J. Nat. Prod. 53, 1362–1364.

Conner, J.M., Gray, A.I., Reynolds, T., Waterman, P.G., 1987. Anthraquinone, anthrone and phenyl pyrone components of *Aloe nyeriensis* var. kedongensis leaf exudate. Phytochemistry 26, 2995–2997.

Cuyckens, F., Claeys, M., 2004. Mass spectrometry in the structural analysis of flavonoids. J. Mass Spectrom. 39, 1–15.

Davis, R.H., Rosental, K.Y., Cesario, L.R., Rouw, G.A., 1989. Processed *Aloe vera* administered topically inhibits inflammation. J. Am. Podiatry Med. Assoc. 79, 395–397.

Durì, L., Morelli, C.F., Crippa, S., Speranza, G., 2004. 6-Phenylpyrones and 5-methylchromones from Kenya *Aloe*. Fitoterapia 75, 520–522.

El-Hela, A.A., Al-Amier, H.A., Ibrahim, T.A., 2010. Comparative study of the flavonoids of some *Verbena* species cultivated in Egypt by using high-performance liquid chromatography coupled with ultraviolet spectroscopy and atmospheric pressure chemical ionization mass spectrometry. J. Chromatogr. A 1217, 6388–6393.

El Maggar, E.B., 2012. Artemisia herba alba and *Artemisia monosperma*: the discovery of the first potential Egyptian plant sources for the pharmaceutical commercial production of artemisinin and some of its related analogues. J. App. Pharm. Sci. 2, 77–91.

Eshun, K., He, Q., 2004. *Aloe vera*: a valuable ingredient for the food, pharmaceutical and cosmetic industries – a review. Crit. Rev. Food Sci. Nutr. 44, 91–96.

Ferreres, F., Gill-Izquierdo, A., Andrade, P.B., Valentao, P., Tomas-Barberan, F.A., 2007. Characterization of *C*-glycosyl flavones *O*-glycosylated by liquid chromatography–tandem mass spectrometry. J. Chromatogr. A 1161, 214–223.

Gobbo-Neto, L., Lopes, N.P., 2008. Online identification of chlorogenic acids, sesquiterpene lactones, and flavonoids in the Brazilian arnica *Lychnophora ericoides* Mart. (Asteraceae) leaves by HPLC–DAD–MS and HPLC–DAD–MS/MS and a validated HPLC–DAD method for their simultaneous analysis. J. Agric. Food Chem. 56, 1193–1204.

Gouveia, S.F., Castilho, P., 2011. Characterisation of phenolic acid derivatives and flavonoids from different morphological parts of *Helichrysum obconicum* by a RP-HPLC–DAD(−)–ESI-MS n method. Food Chem. 129, 333–344.

Grace, O.M., Simmonds, M.S.J., Smith, G.F., Van Wyk, A.E., 2010. Chemosystematic evaluation of *Aloe* section Pictae (Asphodelaceae). Biochem. Syst. Ecol. 38, 57–62.

Grace, O.M., Kokubun, T., Veitch, N.C., Simmonds, M.S.J., 2008. Characterisation of a nataloin derivative from *Aloe ellenbeckii*, a maculate species from east Africa. South Afr. J. Bot. 74, 761–763.

Hirata, T., Suga, T., 1978. Structure of aloenin, a new biologically-active bitter glucoside from *Aloe arborences* var. *natalensis*. Bull. Chem. Soc. Jpn. 51, 842–849.

Holzapfel, C.W., Wessels, P.L., Wyk, B.V., Marais, W., Portwig, M., 1997. Chromone and aloin derivatives from *Aloe broomii*, *A. africana* and *A. speciosa*. Phytochemistry 45, 97–102.

Hutter, J.A., Salmon, M., Stavinoha, W.B., Satsangi, N., Williams, R.F., Streeper, R.T., Weintraub, S.T., 1996. Anti-inflammatory *C*-glucosyl chromone from *Aloe barbadensis*. J. Nat. Prod. 59, 541–543.

Imanishi, K., Ishiguro, T., Saito, H., Suzuki, I., 1981. Pharmacological studies on a plant lectin, Aloctin A. I. Growth inhibition of mouse methylcholanthrenine-induced fibrosarcoma (MethA) in ascites form by Aloctin A. Experimentia 37, 1186–1187.

Jaffer, A.J., Mahmoud, M.J., 2011. Isolation and identification of three flavonoids from *Artemisia* herba-alba (Asteraceae). Al-Mustansiriyah J. Sci. 22, 214–221.

Lau, T.W., Sahota, D.S., Lau, C.H., Chan, C.M., Lam, F.C., Ho, Y.Y., Fung, K.P., Lau, C.B.S., Leung, P.C., 2008. An *in vivo* investigation on the wound-healing effect of two medicinal herbs using an animal model with foot ulcer. Eur. Sur. Res. 41, 15–23.

Lee, K.Y., Weintraub, S.T., Yu, B.P., 2000. Isolation and identification of a phenolic antioxidant from *Aloe barbadensis*. Free Radic. Biol. Med. 2, 261–265.

Luo, J., Nishiyama, Y., Fuell, C., Taguchi, G., Elliott, K., Hill, L., Tanaka, Y., Kitayama, M., Yamazaki, M., Bailey, P., Parr, A., Michael, A.J., Saito, K., Martin, C., 2007. Convergent evolution in the BAHD family of acyl transferases: identification and characterization of anthocyanin acyl transferases from *Arabidopsis thaliana*. Plant J. 50, 678–695.

Matern, U., Heller, W., Himmelspach, K., 1983. Conformational changes of apigenin 7-*O*-(6-*O*-malonylglucoside), a vacuolar pigment from parsley, with solvent composition and proton concentration. Eur. J. Biochem. 133, 439–448.

Mebe, P.P., 1987. 2′-*p*-Methoxycoumaroylaloeresin, a *C*-glucoside from *Aloe excelsa*. Phytochemistry 26, 2646–2647.

Meredova, G.K.H., Nikonov, G.K., Davydova, R.A., 1973. Izv. Akad. Navk. Turkm.-SSR. Ser. Biol. Nauk 6, 71–79.

Newton, I.E., 2004. Aloes in habitat. In: Reynolds (Ed.), Aloes: The Genus Aloe. CR Press, pp. 3–14.

Okamura, N., Hine, N., Tateyama, Y., Nakazawa, M., Fujioka, T., Mihashi, K., Yagi, A., 1998. Five chromones from *Aloe vera* leaves. Phytochemistry 49, 219–223.

Oldfield, S.A., 2004. Review of significant trade: east African aloes. Document 9.2.2 Annex 4, Fourteenth meeting of the Plant Committee, Windhoek, 16–20 February 2004. Convention on International Trade in Endangered Species of Wild Fauna and Flora, Geneva.

Osol, A., Pratt, R., Gennaro, A.R., 1973. The Unites States Dispensatory. J.B. Lippincott Co., Philadelphia, pp. 46–49.

Patel, D.K., Patel, K., Tahilyani, V., 2012. Barbaloin: a concise report of its pharmacological and analytical aspects. Asian Pac. J. Trop. Biomed. 10, 835–838.

Petroviciu, I., Albu, F., Medvedovici, A., 2010. LC/MS and LC/MS/MS based protocol for identification of dyes in historic textiles. Microchem. J. 95, 247–254.

Piccinelli, A.L., Mesa, M.G., Armenteros, D.M., Alfenso, M.A., Arevalo, A.C., Campone, L., Rastrelli, L., 2008. HPLC–PDA–MS and NMR characterization of *C*-glycosyl flavones in a hydroalcoholic extract of *Citrus aurantifolia* leaves with antiplatelet activity. J. Agric. Food Chem. 56, 1574–1581.

Reynolds, T., 1997. Comparative chromatographic patterns of leaf exudate components from *Aloe* section Pachydendron Haw. Bot. J. Linn. Soc 125, 45–70.

Reynolds, T., 1985. The compounds in Aloe leaf exudates, a review. Bot. J. Linn. Soc. 90, 90–157.

Rowson, J.M., Daglish, C., Fairbairn, W., Gartside, B., Johnson, C.A., Perry, H.M., Ryan, N.A., Swann, R.V., Shallis, P.W., 1967. The chemical assay of Aloes. Analyst (London) 92, 593–596.

Steenkamp, V., Stewart, M.J., 2007. Medicinal applications and toxicological activities of *Aloe* products. Pharm. Biol. 45, 411–420.

Surowiec, I., Szostek, B., Trojanowicz, M., 2007. HPLC–MS of anthraquinoids, flavonoids, and their degradation products in analysis of natural dyes in archaeological objects. J. Sep. Sci. 30, 2070–2079.

Teradaira, R., Shinzato, M., Beppu, H., Fujita, H., 1993. Antigastric ulcer effects in rats of *aloe arborescens* miller var. *natalensis* berger extract. Phytother. Res. 7, S34–S36.

Vallverdú-Queralt, A., Jáuregui, O., Medina-Remón, A., Andrés-Lacueva, C., Lamuela-Raventós, R.M., 2010. Improved characterization of tomato polyphenols using liquid chromatography/electrospray ionization linear ion trap quadrupole orbitrap mass spectrometry and liquid chromatography/electrospray ionization tandem mass spectrometry. Rapid Commun. Mass Spectrom. 24, 2986–2992.

Van Heerden, F.R., Van Wyk, B.E., Viljoen, A.M., 1996. Aloeresins E and F, two chromone derivatives from *Aloe peglerae*. Phytochemistry 43, 867–869.

Van Heerden, F.R., Viljoen, A.M., van Wyk, B.E., 2000. 6′-*O*-Coumaroylaloesin from *Aloe castanea* – a taxonomic marker for *Aloe* section *Anguialoe*. Phytochemistry 55, 117–120.

Viljoen, A.M., Van Wyk, B.E., 2001. A chemotaxonomic and morphological appraisal of *Aloe* series Purpurascentes, *Aloe* section Anguialoe and their hybrid, *Aloe broomii*. Biochem. Syst. Ecol. 29, 621–631.

Wabuyele, E., (Ph.D. dissertation) 2006. Studies on Eastern African Aloes: Aspects of Taxonomy, Conservation and Ethnobotany. University of Oslo.

Wang, W., Cuyckens, F., Heuvel, H.V.D., Apers, S., Pieters, L., Steenkamp, V., Stewart, M.J., Luyckx, V.A., Claeys, M., 2003. Structural characterization of chromone *C*-glucosides in a toxic herbal remedy. Rapid Commun. Mass Spectrom. 17, 49–55.

Winter, C.A., Risley, E.A., Nuss, G.W., 1962. Carrageenan induced oedema in hind paws of the rats as an assay for anti-inflammatory drugs. Proc. Soc. Exp. Biol. Med. 111, 544–557.

Wojakowska, A., Muth, D., Narozna, D., Madrzak, C., Stobiecki, M., Kachlicki, P., 2013. Changes of phenolic secondary metabolites profiles in the reaction of narrow leaf lupin (*Lupinus angustifolius*) plants to infection with Colletotrichum lupine fungus or treatment with its toxin. Metabolomics 9, 575–589.

Wolfson, E.C., Gutterman, Y., 2009. Aloes. Homonataloin and aloenin are important bioactive components for use in cosmetic and medicinal industries. Planta Med. Congress Abstract, http://dx.doi.org/10.1055/s-0029-1234481.

Yagi, A., Kanbara, T., Morinobu, N., 1987. Inhibition of mushroomtyrosinase by *Aloe* extract. Planta Med. 53, 509–582.

Yeats, J., 1870. The Natural Histroy of Commerence. Cassell, Petter and Galpin, London.

Yu, X.H., Chen, M.H., Liu, C.J., 2008. Nucleocytoplasmic-localized acyl transferases catalyze the malonylation of 7-*O*-glycosidic (iso) flavones in *Medicago truncatula*. Plant J. 55, 382–396.